Piezoresistive disposable weight sensor with increased sensitivity

Kuter ERDİL[ID], **Tuğçe AYRAÇ**[ID], **Ö. Gökalp AKCAN**[ID], **Y. Dağhan GÖKDEL**[*][ID]
Department of Electrical and Electronics Engineering, Faculty of Engineering, İstanbul Bilgi University,
İstanbul, Turkey

Abstract: This study presents the design, simulation, implementation, and experimental characterization of a paper-based perforated disposable weight sensor system with a double piezoresistive layer. The demonstrated system is designed to achieve highly sensitive weight sensing operations with low-cost materials. For that purpose, the main fabrication material of the proposed disposable sensor is selected as a 289-μm-thick Strathmore 400 series Bristol paper. Approximately 48-μm-thick piezoresistive graphite paste is coated onto both sides of the paper-based cantilever beam with the aim of acquiring more sensitive weight-sensing capability. Additionally, the proposed paper-based structure has rows of closely spaced perforations at prespecified locations to facilitate the bending of the cantilever beam and to further increase the sensitivity of the system. A peripheral electronic read-out circuitry is developed and integrated into the system. It is experimentally demonstrated that the proposed weight-sensing system can measure miniature weights ranging to 2 g with a resolution of 20 mg. The implemented sensor has a sensitivity of 17.13 mV/mN or 168.01 mV/g.

Key words: Weight sensor, piezoresistive sensor, paper substrate, perforated-structure, disposable sensor, read-out circuitry

1. Introduction

Today, there is a gradually increasing need for disposable and low-cost but sufficiently sensitive and robust sensors. In this vein, this work presents a paper-based perforated sensor that is developed together with its pertinent electronic read-out system as a low-cost and disposable device for the purpose of sensing of microweights and micropressures. The presented weight-sensing system is designed to be cheap and fabricated using a disposable material (Strathmore 400 series Bristol paper), and, most crucially, it aims to perform highly sensitive and robust weight/pressure-sensing operations.

Thus, in achieving this objective, (1) a piezoresistive graphite layer is carefully formed on both sides of the devised paper-based cantilever beam with the aim of simultaneously forming both tensile and compressive stress when there is bending due to the exerted weight. These two inversely altering resistance values are directly utilized to substantially unbalance the Wheatstone bridge circuit that is a part of the electronic read-out circuitry. Moreover, (2) the presented paper-based cantilever device has rows of closely spaced perforations where the applied stress due to weight exertion reaches its maximum value in order to promote the bending of the device and to further increase the sensitivity of the system. Finally, (3) a peripheral electronic read-out circuitry that harbors a Wheatstone bridge circuit with two oppositely changing resistors and an instrumentation amplifier is integrated into the weight-sensing system.

*Correspondence: daghan.gokdel@bilgi.edu.tr

It is a well-known fact that Si-based sensors and devices need relatively long and expensive fabrication processes that are usually performed in clean-room environments. Today, alternative fabrication methods and materials are specifically required where quick and cheap prototyping becomes a necessity. Various disposable MEMS sensors are reported in the literature. Utilization of polymer materials as the main fabrication material is one of the most frequently preferred methods for low-cost disposable sensors.

A flexible polyimide-based force sensor was previously described, where polyimide is employed both as a flexible substrate and as an elastic dielectric material [1]. There are also proposed systems that employ polydimethylsiloxane (PDMS) as a base fabrication material for flexible capacitive tactile sensors [2]. Furthermore, materials such as ionic polymer metal composites (IPMCs) [3], polydimethylsiloxane (PDMS) [4], SU8 [5], parylene [6], PVDF [7, 8], conducting polymers [9, 10], and polymers [11–15] are preferred for mostly tactile and pressure sensor fabrication.

A good alternative to cheap and flexible polymer fabrication materials is generic paper owing to its abundance, easy accessibility, and suitability to fabricate low-cost sensing devices in a very quick manner. In the literature various sensors implemented using paper as the main fabrication material have been reported [16–23].

It should be stated once again that the main aim of this work is to develop a low-cost weight sensor with increased sensitivity. Therefore, a piezoresistive sensing mechanism is preferred to delicately sense the change in weight occurring at tip of the paper-based cantilever beam. Lately, there have been many reported low-cost tactile, pressure, and force and biosensing devices that use the piezoresistive sensing mechanism [24–27]. It was also demonstrated that carbon nanotubes together with an epoxy composite can be used as a piezoresistive pressure sensor having sensitivity of 13 kPa^{-1} [28].

The remainder of this paper is organized as follows. First, the operation principle of the proposed system is thoroughly explained in Section 2. Afterwards, in Section 3 and in Section 4, the proposed cantilever beam design is elaborated and then simulated using finite-element method software, respectively. After describing the implementation process of the sensing device in Section 5, the electronic read-out circuit is explained in the following section. The paper is concluded by sharing the acquired experimental results in Section 7 and a comprehensive discussion in Section 8.

2. Operation principle

The designed weight-sensing system harbors three essential components. These are a disposable paper-based weight sensor, a simple read-out circuitry that is able to detect small changes in resistance stemming from stress occurring on the piezoresistive graphite layer, and a generic multimeter (Agilent 34450A). The underlying operation principle of the proposed system is illustrated in Figure 1.

The proposed paper-based fixed-free cantilever beam whose top and bottom surfaces at the anchor point are coated with thin-film piezoresistive graphite layers is directly bent in the direction of the point-force $\vec{F}$ that is exerted to the tip of the structure as delineated in Figure 1. The formula describing this relation between tip-displacement δ_c of the cantilever beam and the applied point-force $|F|$ is given in Equation 1 from [29]:

$$\delta_c = \frac{4|F|L_c^{\,3}}{Ew_ct_c^{\,3}}, \tag{1}$$

where E, w_c, L_c, and t_c correspond to Young's modulus of the main fabrication material and to the
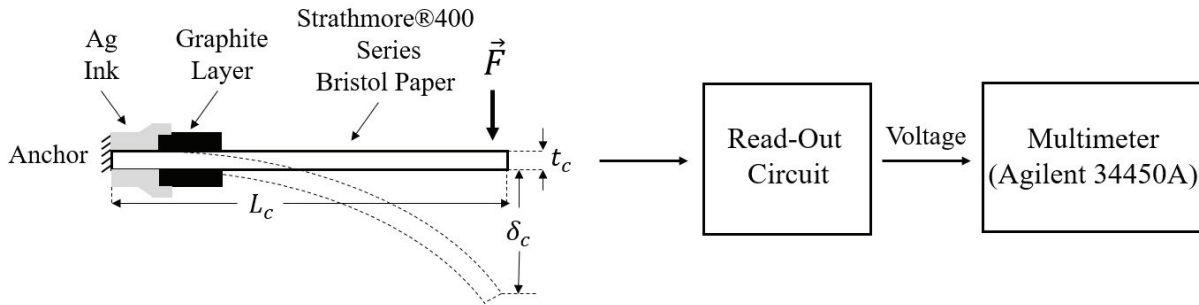
Figure 1. System diagram of the proposed weight-sensing system. System harbors a paper-based sensor along with a read-out circuit and a multimeter. Total resistance change arising from the applied force to tip of the cantilever beam is detected and then amplified using the implemented read-out circuitry and subsequently fed into a multimeter.

width, length, and thickness of the cantilever beam, respectively. The tip-displacement δ_c, whose magnitude increases linearly with the amplitude of the exerted force, simultaneously creates both a tensile stress on the top piezoresistive graphite layer and a counter compressive stress on the bottom surface of the graphite layer (or vice versa) depending on the direction of the applied force. The maximum stress, σ_{max}, occurring on the graphite layer is given in Equation 2 [29–31]. Assuming that the thickness of the proposed sensing structure, t_c, is identical to the thickness of the main fabrication material, it can be said that one can carefully choose an optimal value for length L_c and width w_c of the proposed cantilever beam structure and attain a considerable amount of augmentation in tensile and compressive stresses that are formed on the top and bottom piezoresistive layers as shown in Figure 1. Maximum stress occurs at the fixed end of the cantilever and its magnitude linearly decreases towards the deflected end [30]:

$$\sigma_{max} = \frac{6|F|L_c}{w_c t_c^{\,2}}. \tag{2}$$

In conjunction with alternating mechanical stress, a resistance change of ΔR arises for each (top and bottom) piezoresistive graphite layer. These related resistance changes are detected and subsequently amplified using a single read-out circuitry that is simply composed of a Wheatstone bridge circuit and an instrumental amplifier (INA128). Acquired voltage signals are then delivered to a generic multimeter (Agilent 34450A), which ultimately ensures an accurate sensing of the applied force.

3. Proposed design

Figure 2 illustrates the proposed perforated paper-based weight sensor. Critical design parameters affecting the performance of the structure are precisely shown in the figure. The related values of these design parameters are given in Table 1. The paper-based sensing structure is designed in a such a way that the disposable device has an uncomplicated clean geometry easing the following fabrication and measurement steps. Therefore, a generic simple cantilever geometry is chosen for this study. Secondly, the stress occurring due to the applied force on the tip of the structure should be maximized in order to increase the sensitivity (mV/g). Therefore, the width w_{c_1} of the cantilever beam is continuously enlarged to w_{c_2} as we move through the cantilever beam, from the anchor to the tip-point, as shown in Figure 2a. This rise ensures a shift in the location of the center of the mass of the structure towards the tip, consequently creating an augmentation in the stress level. Finally, the

structure is designed to have its maximum stress formed in the direction of $A - A'$ as demonstrated in Figure 2a.
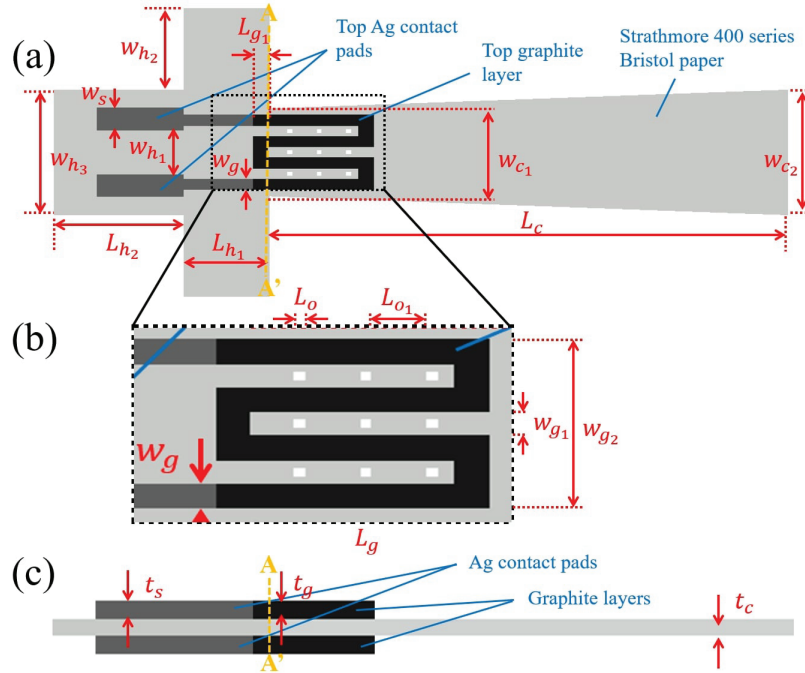

Figure 2. Technical illustration of the proposed sensing structure showing the design parameters: (a) top view of the structure, (b) close-up view of the perforated structure together with the graphite layer, (c) side view of the proposed sensing structure.

Table 1. Parameters and values of proposed design illustrate in Figure 2.

Parameters	Values (mm)	Parameters	Values (mm)
L_c	30	w_{g_1}	0.9
w_{c_1}	7	w_{g_2}	5.5
w_{c_2}	10	t_g	0.5
t_c	0.289	L_{o_1}	1.4
L_{h_1}	5	L_o	0.3
w_{h_1}	3.5	w_o	0.3
L_{h_2}	7.49	L_{g_1}	1
w_{h_2}	5	w_g	0.7
w_{h_3}	10	t_s	0.5
L_g	7	w_s	1.8

In order to benefit from the accumulating stress in the $A - A'$ direction, a serpentine-shaped piezoresistive layer is preferred at that location as depicted in Figure 2b. The resistor that is composed of the above-mentioned serpentine-shaped piezoresistive graphite film with a thickness of 50 μm is precisely positioned 1 mm away from the fixed end of the paper-based structure with the main aim of optimally harvesting the resistance change. As Table 1 elaborates, the length (L_g), width (w_{g_2}), and thickness (t_g) of this layer are chosen as 700 μm,

550 μm, and 50 μm, respectively. The tip of cantilever beam is designed to have an area of size proportionate to the apex of an index finger in order to facilitate the subsequent force-displacement characterization process. Therefore, the width of the tip of the cantilever (w_{c_2}) is selected as 10 mm. Moreover, in order to get the minimum possible width for the fixed end w_{c_1} of the proposed cantilever beam and choose meaningful puncture sizes, or in other words, for increasing the stress created at the anchor point, the sensitivity, minimum feature sizes, and fabrication limits were investigated. In that vein, the line width of the graphite layers (w_g) is chosen to be 700 μm, while dependently the width of the fixed end of the cantilever beam (w_{c_1}) is selected as 7 mm and finally the technology-limited puncture size ($L_o \times w_o$) is preferred to be 400 μm $\times$ 400 μm. Afterwards, every other parameter that is tabulated in Table 1 is carefully selected in conjunction with the initial choice of w_{c_2} without being oblivious to possible fabrication errors and the technology limits of our implementation process, which will be elaborated in Section 6.

Moreover, as illustrated in Figure 2a, there exists two nonoperational ears that are placed at the right- and left-hand sides of the Ag contact pads. These redundant surfaces are used to immobilize the structure onto the printed circuit board harboring the peripheral electronics circuits and to ensure a robust operation.

4. Simulation results

In the following step, the proposed designs are simulated to examine their performance. Figures 3 and 4 illustrate these finite-element method (FEM) simulations of the various perforation patterns.
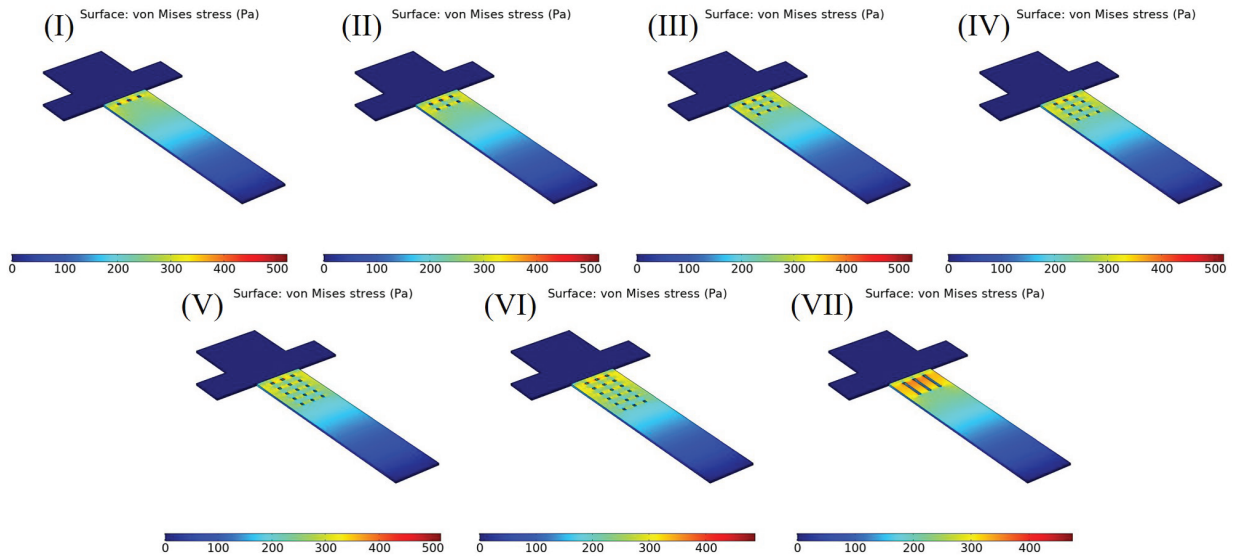

Figure 3. Finite-element method simulation results of various perforation patterns for sensing structures showing the maximum stress values at the fixed end of the cantilever.

The main objective of these simulations is to evaluate which puncture topology has a stronger effect on augmenting the stress (σ_{max}) at the anchor assuming a constant weight value (0.1 mg) exerted onto the tip of the cantilever beam. Pertinent simulation results are tabulated in Table 2. At this point, it is critical to indicate that the puncture sizes are chosen considering the fabrication resolution and capabilities of the laser cutter that is used. The resolution of the Epilog Helix 24, 60 W, is tested and it is determined that a minimum of $400\,\mu$m $\times 400\,\mu$m squares can be laser-cut without over-burning the edges.
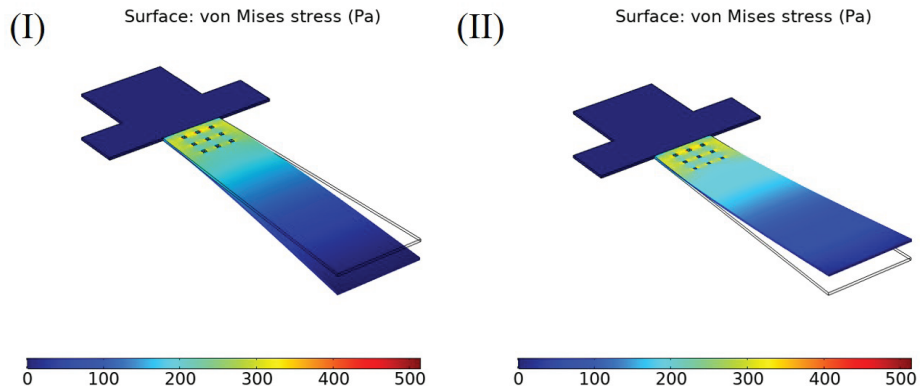
Figure 4. Simulation results of compressive (I) and tensile (II) behavior enlarging the perforated cantilever beam. Maximum stress value is observed as 518 Pa with 240.27 nm tip displacement. View of the stress density distribution on the paper-sensing structure as a result of applied weight to tip and its tip displacement are marked.

Table 2. FEM simulation results for various perforation patterns.

Design number	Puncture size (μm $\times$ μm)	Array size	Anchor stress (Pa)	Tip displacement (nm)
I	400$\times$ 400	3$\times$ 1	518	257.77
II	400$\times$ 400	3$\times$ 2	515	260.36
III	400$\times$ 400	3$\times$ 3	525	262.64
IV	400$\times$ 400	3$\times$ 4	516	264.66
V	400$\times$ 400	3$\times$ 5	514	266.30
VI	400$\times$ 400	3$\times$ 6	513	267.75
VII	400$\times$ 3800	3$\times$ 1	474	277.60

As can be deduced from the simulation results tabulated in Table 2, as the array size gets larger, the stress occurring at the anchor exhibits almost an inverted U-curve behavior, whereas the tip displacement of the cantilever beam continuously increases from approximately 257.77 nm to 277.60 nm. Even though acquiring a stress value as large as possible at the anchor for an applied force is the desired effect, one should also scrutinize the increase in tip displacement value and prevent the unnecessary bending of the cantilever beam. The reason for this consideration is twofold. First, the initial bending/displacement of the cantilever beam without exertion of external force must be negligible so that the final product will have a larger dynamic range of sensing. Secondly, having a larger initial bending affects the equilibrium between initial resistance values of the top (tensile) and bottom (compressive) piezoresistive layers, which are assumed to be equal for the subsequent electronic read-out circuit. For these reasons, design number III is selected as the optimum one since it not only keeps the balance between initial resistance values but also ensures a considerable increase of anchor-stress for an externally applied force.

Lastly, Figure 4 shows the FEM simulation results of the final proposed design for the paper-based sensing structure whose dimensions are tabulated in Table 1. It must be stated that this paper-based sensing structure uses a 3$\times$3 puncture array with a puncture size of 400 μm$\times$ 400 μm. It is shown through the simulation that exerting 0.1 mg onto this structure produces a stress value of 518 Pa at the anchor point where the piezoresistive layer lies.

5. Implementation

Figure 5 shows various steps of the fabrication process of our proposed perforated paper-based disposable weight sensor. In this work, as the main fabrication material and the method, a 289-μm-thick Strathmore 400 series Bristol paper and screen-printing are preferred. The predicted final conceptual view of the proposed sensing structure having two separate graphite layers located on the top and bottom surfaces of the paper cantilever beam, along with their Ag contact pads, is depicted in Figure 5 (inset I). As the first step, the silk stencil mask (mask I) shown in inset II-a having a pore size of 36 μm and an approximate thickness of 48 μm is utilized to apply the graphite paste onto both sides of the paper. In this work, an electrically highly resistant graphite paste (Bare Conductive ink, 55 Ω/Sq @ 50 microns) was selected considering its good adhesion and nontoxic, water-soluble properties. Graphite paste is skillfully applied to the Bristol paper by means of a rubber brush as depicted in inset II-a and 48-μm-thick graphite is coated on the paper-based cantilever beam. Subsequently, silver electrical contact pads are formed resorting to a second stencil mask (mask II) as in Figure 5 (inset II-b), again having the same pore size of 36 μm and approximate thickness of 48 μm together with a low-resistant silver paste (Gwent C2130809D5 Silver:Silver Chloride paste 60:40), which was selected considering its high conductivity and low curing temperature properties. The same prior procedure has been followed as illustrated in inset II-b to coat the electrical contact pads. The Ag layer of roughly 48 μm thick is delicately coated to ensure electrical connectivity between the sensor and the read-out electronic circuitry.
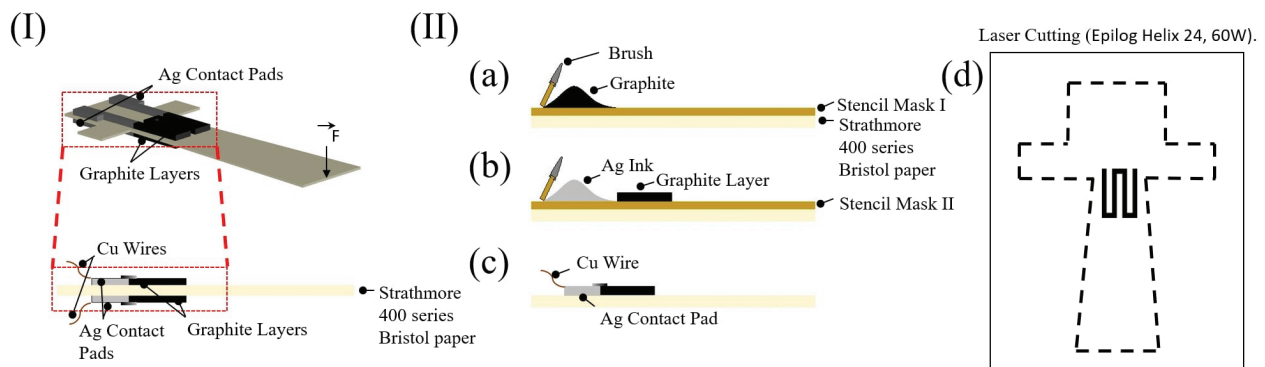

Figure 5. (I) Three dimensional (3D) drawing of the proposed double-side perforated paper-based structure including a graphite layer and Ag contact pads. (II) Fabrication process of the double-side perforated paper-based sensor.

In order to obtain a double-sided structure as elaborated in Section 2, the same process is carefully duplicated on the other surface of the cantilever beam after a sensitive alignment step. In the final step, the cantilever beam is precisely cut employing the help of a laser cutter (Epilog Helix 24, 60 W). The fabrication process is concluded by connecting Cu wires to Ag pads to ensure electrical connectivity as in Figure 5 (inset II-c).

The fabricated perforated paper-based structure is shown in Figure 6a and a close-up view of the top surface of the graphite and Ag-coated structure is shown on the right-hand side of Figure 6b along with its measurement dimensions. Close-up views of the aforementioned stencil mask I and stencil mask I are depicted in Figures 6c and 6d.
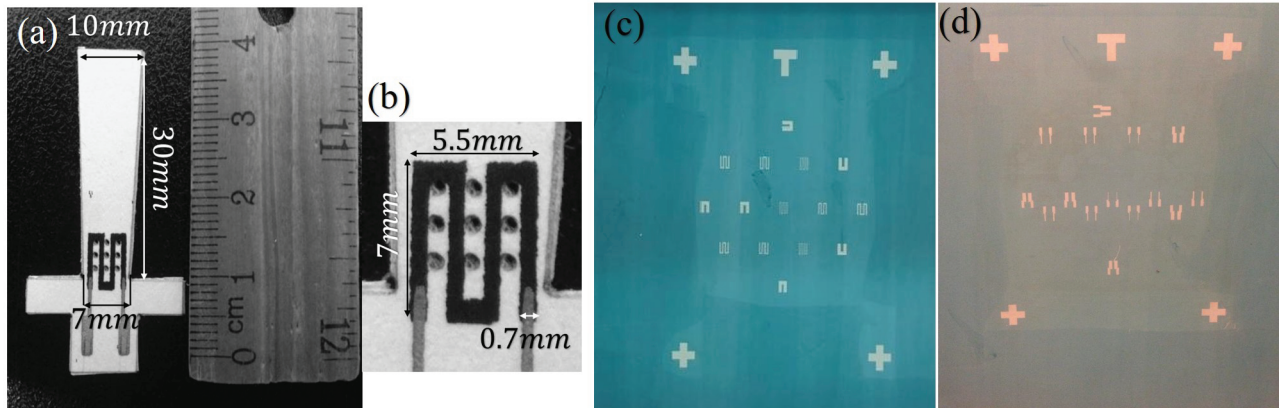
Figure 6. (a) View of the fabricated paper-based force sensor and (b) close-up view of the serpentine piezoresistive layer with $400\,\mu m \times 400\,\mu m$ perforated structures. (c) Close-up view of the graphite layer mask (stencil mask I) and (d) close-up view of the Ag contact pads mask (stencil mask II).

6. Electronic read-out circuitry

As shown in Figure 5, the proposed sensing system has two thin-film graphite layers that are separately coated on the top and bottom surfaces of the same cantilever beam, whereas a typical piezoresistive pressure/weight sensor [16–18] employs just one thin-film layer to detect the resistance changes caused by exerting force through mass $m\vec{g}$. Assuming that the alternating resistance values of the top and bottom graphite layers due to the utilized mass are $+\Delta R$ and $-\Delta R$, one may successively employ Wheatstone bridge circuitry with two varying resistors and then an instrumentation amplifier, as illustrated in Figure 7a, in order to be able to detect the slightest resistance changes $+\Delta R$ and $-\Delta R$ [32]. Output voltage of the proposed read-out system is stated in Equation 3, with G being the gain of the instrumentation amplifier:
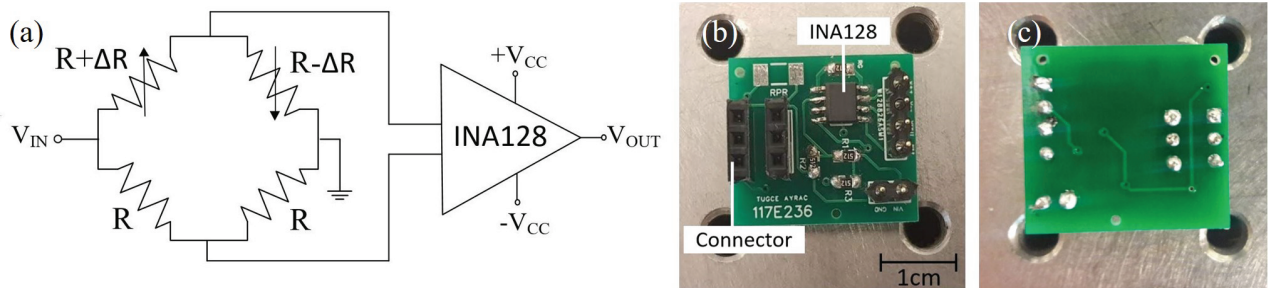

Figure 7. (a) Electronic read-out circuit that consists of a Wheatstone bridge circuit with two inversely changing graphite resistors and a subsequent instrumentation amplifier, INA128, to further amplify the voltage signal acquired trough the resistance change. Top (b) and bottom (c) views of the printed circuit board for the proposed electronic read-out circuit. Implemented PCB has dimensions of 26 mm × 22 mm.

$$V_{OUT} = \frac{V_{IN}}{2}\frac{\Delta R}{R}G. \tag{3}$$

The main objective of the Wheatstone bridge circuit in this system is to detect the unknown value of ΔR, which is actually the resistance change of the thin-film graphite layers [17]. At the beginning, the circuit

calibrates the system output by balancing the two branches of the bridge circuit and by ensuring to initially acquire a zero-volt output when there is no bending. Since the sensing structure begins to be bent and the tip displacement δ_c starts to gradually increase as a consequence of the exerted mass $m\vec{g}$, the value of ΔR begins to augment and correspondingly the circuit becomes unbalanced and an output voltage starts to emerge. As shown in Figure 7a, a Wheatstone bridge circuit having two inversely changing resistors $R + \Delta R$ and $R - \Delta R$ is chosen in this study. Immediately after the mass $m\vec{g}$ acts on the tip of the paper-based cantilever beam, the arising bending forms a tensile and a compressive stress on the top and bottom graphite layers, respectively. These opposing types of stress cause $+\Delta R$ and $-\Delta R$ changes in the proposed circuit [33, 34].
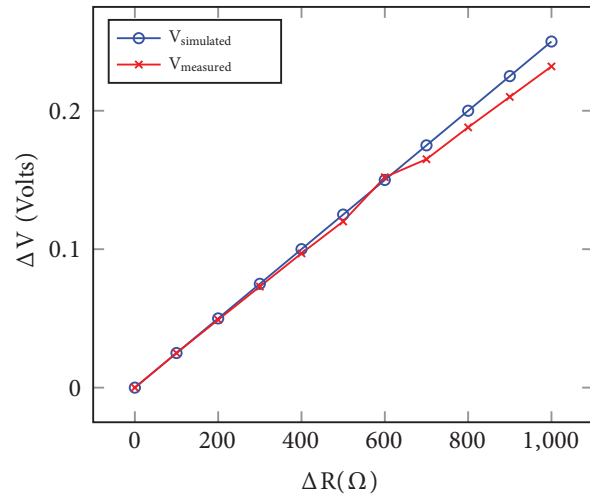

Figure 8. Plot of the output voltage change (ΔV) as a function of resistance change (ΔR). Blue line corresponds to simulation results of proposed read-out circuit, whereas red line corresponds to measurement results of system with implemented PCB.

Distinct from conventional Wheatstone bridge circuits, having two conversely differentiating resistors that unbalance the bridge in the circuit inherently increases the gain of the systems' transfer function by twofold as stated in Equation 3. To further increase the sensitivity of the system, an instrumentation amplifier (INA128) is attached to the output of the Wheatstone bridge circuit [35, 36]. The amplifier is designed to possess a voltage gain of G, which is equal to 100 V/V. The output voltage that is formed at the output of the circuit as a result of increased stress in the graphite piezoresistive layer is then amplified via the instrumentation amplifier and fed into a digital multimeter. The proposed electronic read-out circuit is implemented using surface mount devices as a printed circuit board (PCB) and is shown in Figures 7b and 7c. The length and width of the board are 26 mm and 22 mm, respectively. The proposed electronic read-out circuit is simulated with LTspice software for an increasing value of R and the simulation result is shown in Figure 8 as $V_{simulated}$. It is also tested with an implemented PCB and the measurement result is indicated as $V_{measured}$. On the other hand, the test setup shown in Figure 9a is designed to detect the stress level and corresponding resistance change values caused by the force generated by using different weights at the free end of the paper-based structure. Experimental data are collected by following the same procedure. Figure 10 plots the normalized resistance change $\Delta R/R$ of the proposed weight-sensing systems under the application of an increasing point-force that causes a linear rise of the tip displacement value.
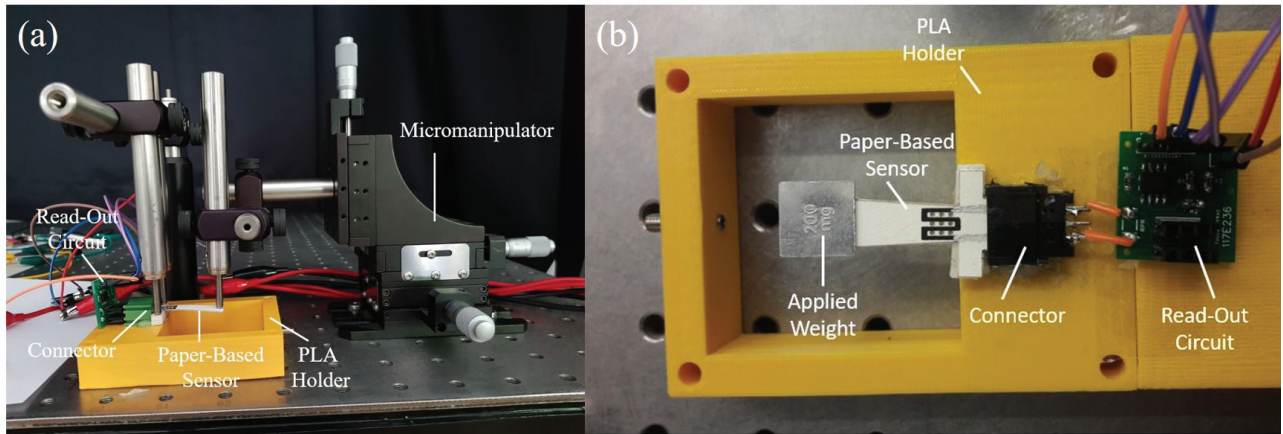
Figure 9. (a) Experimental test setup to monitor the tip displacement versus the normalized resistance change of the proposed sensing system. (b) View of the experimental setup for the proposed force-sensing system with an applied weight.
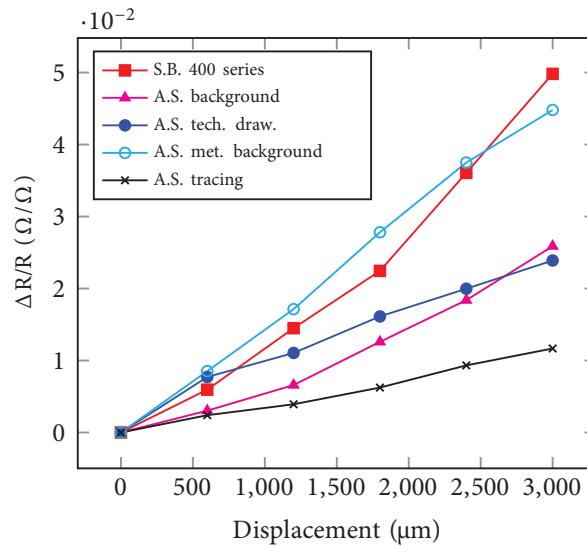

Figure 10. Plot of the normalized resistance change ($\Delta R/R$) for increasing tip displacement (δ_c). Red, pink, blue, cyan, and black lines show that behavior of different papers. They correspond to Strathmore 400 series Bristol paper, Alex Schöller background paper, Alex Schöller technical drawing paper, Alex Schöller metallized background paper, and Alex Schöller tracing paper.

7. Experimental results

In the following step, the proposed sensing system is tested. The test setup that is used to monitor the behavior of the designed and implemented system is shown in Figure 9a. The former shows the devised test setup that monitors the change in resistance occurring in the piezoresistive layer. It was previously explained that the level of resulting stress at the anchor point of the paper-based structure increases in direct proportion to the amount of tip displacement (δ_c) caused by the bending of the paper structure.

As shown in Figure 9a, the paper-based structure is fixed onto a platform using a three-dimensional (3D) printed holder made out of PLA (polylactic acid) filament. The tip displacement at the free-end point of the

paper is formed by means of the micromanipulator, which has motion sensitivity of 5 μm. The paper-based cantilever beam is getting slowly bent through the micromanipulator and dependently the stress value at the anchor is gradually raised. The stress levels and the resistance change values occurring on the graphite layer are transmitted to the read-out circuit through the connector, which is fixed to the PLA holder via Ag contact pads.

In this test, the effects of using different kinds of fabrication materials such as Strathmore 400 series Bristol paper, Alex Schöller background paper, Alex Schöller technical drawing paper, Alex Schöller metallized background paper, and Alex Schöller tracing paper are investigated. When the tip displacement(δ_c) value is gradually increased from 0 to 3000 μm with the help of the micromanipulator as indicated in Figure 9a, normalized resistance change (ΔR/R) of the Strathmore 400 series Bristol paper is monitored and it is seen that the normalized resistance change linearly increases from 0 to 0.04982 Ω/Ω as emphasised in Figure 10.

Moreover, it is also reported for the other cantilever beams that when their tip displacements (δ_c) are increased from 0 to 3000 μm, normalized resistance changes (ΔR/R) increase from 0 to 0.02588 Ω/Ω, 0.02389 Ω/Ω, 0.04480 Ω/Ω, and 0.01167 Ω/Ω for Alex Schöller background paper, Alex Schöller technical drawing paper, Alex Schöller metallized background paper, and Alex Schöller tracing paper, respectively, as shown in Figure 10.

According to the test results, the Strathmore 400 series Bristol paper having magnitude of 0.04982 Ω/Ω, which is the maximum normalized resistance change (ΔR/R) value without having any plastic deformation for the paper-based structure, is selected among all the other paper-based fabrication materials. Furthermore, Figure 11 plots the alternating normalized resistance changes versus the tip displacement with an emphasis on the effect of changing piezoresistive layers both in number and topology. In this plot, the change in the negative direction represents the resistance change due to compressive stress, whereas the change in the positive direction corresponds to the change in resistance through tensile stress. As the experimental results show, the single-serpentine piezoresistive layer design is stable and linear, but on the other hand it has a similar sensitivity compared to the double-serpentine structure. Thus, we resorted to the single-serpentine shaped piezoresistive layer in the final implementation.

8. Discussion

The aim of this study is to design and manufacture a paper-based disposable weight sensor with improved sensitivity. Numerous fabrication methods and materials are compared in the literature. It that vein, it has been reported that the paper-based structures are more suitable for creating disposable devices since they are easy to fabricate, abundant, and cheap.

As elucidated above, in this work, we propose a quick-to-fabricate paper-based, perforated cantilever beam having two single-serpentine shaped piezoresistive layers to measure applied weight. Figure 12 clearly shows that the perforated sensor having a double-sided piezoresistive layer has a higher sensitivity level (17.13 mV/mN) compared to the generic nonperforated paper-based sensor with a single sensing layer (0.84 mV/mN). In this work, the sensitivity of a simple paper-based weight sensor [17] is improved almost 20 times using the proposed methods. The sensitivity of a cheaper paper-based sensor used with old-fashioned and unrepeatable fabrication methods [18] is enhanced almost 19 times using ours. A concise comparison between this work and the works reported in [17] and [18] is tabulated in Table 3.
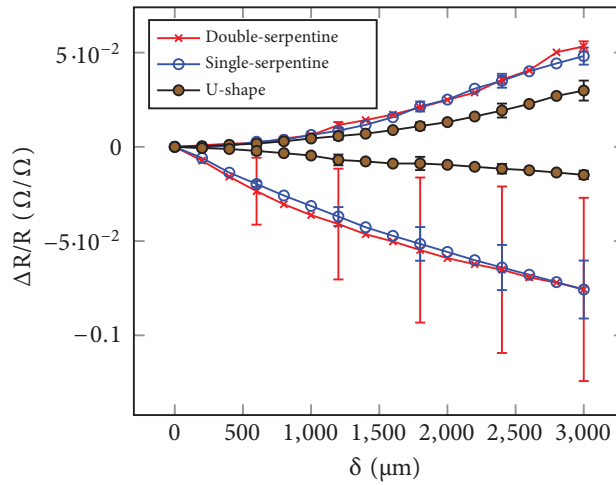
Figure 11. Plot of the normalized resistance change for increasing tip displacement. Since the proposed sensing structure has two piezoresistive layers, one being located above and the other below the paper-based structure, the plots are almost symmetrical along the ΔR/R=0 line considering the opposing stresses (tensile and compressive) forming in respective layers.
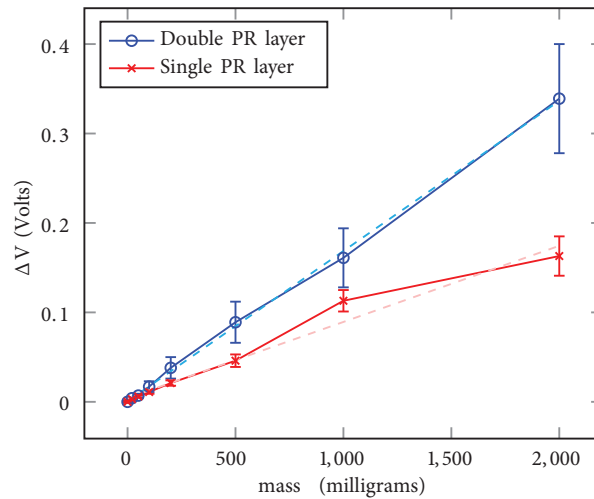

Figure 12. Plot of the output voltage change (ΔV) as a function of the applied mass. Red line corresponds to mass-dependent voltage change of a paper-based sensor with a single-sided screen-printed piezoresistive (PR) layer, whereas blue line corresponds to the one with a two-side screen-printed piezoresistive layer. The one having a double-sided PR layer has 168.01 mV/g (=17.13 mV/mN) sensitivity, whereas the one with the single-sided PR layer has 85.13 mV/g (=8.68 mV/mN) sensitivity.

9. Conclusion

In this work, a paper-based perforated disposable weight sensor system with double piezoresistive layer has been designed, fabricated, and characterized along with the peripheral electronic circuit. The demonstrated system is designed to achieve a highly sensitive weight-sensing operation with low-cost materials. For that purpose, the main fabrication material of the proposed disposable sensor is chosen as 289-μm-thick Strathmore 400 series Bristol paper. Approximately 48-μm-thick piezoresistive graphite paste is coated onto both sides of the paper-based cantilever beam with the aim of acquiring more sensitive weight-sensing capability. Additionally,

Table 3. Comparison of specifications of our paper-based weight sensor to the works in [17] and [18].

Specifications	This Work	Reference [17]	Reference [18]
1. Substrate	Strathmore 400 series Bristol paper (289 μm thick)	Whatman 3MM chromatography paper (340 μm thick)	A4 paper (88 μm thick)
2. Pattern method for substrate	Laser equipment	Laser equipment (Epilog Helix 24, 60 W)	Scissors
3. Beam size $L \times (w_1 - w_2) \times t$	30 mm × (7-10 mm) × 0.289 mm	44.5 mm × 7.7 mm × 0.34 mm	45 mm × 8 mm × 0.088 mm
4. Young's modulus	2.388 GPa	$1.98 \pm 0.17\ GPa$	0.03 GPa
5. Force & mass ranges	2 g (19.6 mN)	16 mN	50 mN
6. Force & mass resolutions	20 mg (196 μN)	120 μN	500 μN
7. Sensitivity	168.01 mV/g (17.13 mV/mN)	0.84 mV/mN	0.9 mV/mN
8. Sensing material	Graphite (Bare Conductive Electric Paint)	Graphite ink	Graphite pencil
9. Pattern method for sensing material	Silk screen-printing	Silk screen-printing	Hand-drawing
10. Electrode material	Ag ink (Gwent C2130809D5:Silver Chloride paste 60:40)	Ag ink	Copper foil
11. Fabrication process	<10 min in laboratory	<1 h in laboratory	<30 min in any place
12. Device cost	<\$0.04 per device	\$0.04 per device	\$0.01 per device

the proposed paper-based structure has rows of closely spaced perforation at prespecified locations to facilitate the bending of the cantilever beam and to further increase the sensitivity of the system. A peripheral electronic read-out circuitry is developed and integrated into the system. It is experimentally demonstrated that the proposed weight-sensing system can measure miniature weights ranging to 2 g with a resolution of 20 mg and costs under \$0.04 per device. The implemented sensor has sensitivity of 17.13 mV/mN or 168.01 mV/g. We showed that the sensitivity of a simple paper-based weight sensor is improved almost 20 times using the proposed methods.

Acknowledgment

References

[1] Dobrzynska JA, Gijs MAM. Flexible polyimide-based force sensor. Sensors and Actuators A: Physical 2012; 173 (1): 127-135. doi: 10.1016/j.sna.2011.11.006

[2] Lee HK, Chung J, Chang SI, Yoon E. Normal and shear force measurement using a flexible polymer tactile sensor with embedded multiple capacitors. Journal of Microelectromechanical Systems 2008; 17 (4): 934-942. doi: 10.1109/JMEMS.2008.921727

[3] Bonomo C, Fortuna L, Giannone P, Graziani S, Strazzeri S. A resonant force sensor based on ionic polymer metal composites. Smart Materials and Structures 2007; 17 (1): 015014. doi: 10.1088/0964-1726/17/01/015014

[4] Lee, HK, Chung J, Chang SI, Yoon E. Real-time measurement of the three-axis contact force distribution using a flexible capacitive polymer tactile sensor. Journal of Micromechanics and Microengineering 2011; 21 (3): 035010. doi: 10.1088/0960-1317-21-3-035010.

[5] Hasenkamp W, Forchelet D, Pataky K, Villard J, Van LH et al. Polyimide/SU-8 catheter-tip MEMS gauge pressure sensor. Biomedical Microdevices 2012; 14 (5): 819-828. doi: 10.1007/s10544-012-9661-8

[6] Crum B, Li W. Parylene-based fold-and-bond wireless pressure sensor. In: The 8th Annual IEEE International Conference on Nano/Micro Engineered and Molecular Systems; Suzhou, China; 2013. pp. 1155-1158.

[7] Su YF, Kotian RR, Lu N. Energy harvesting potential of bendable concrete using polymer based piezoelectric generator. PComposites Part B: Engineering 2018; 153: 124-129. doi: 10.1016/j.compositesb.2018.07.018

[8] Wang X, Sun F, Yin G, Wang Y, Liu B, Dong M. Tactile-sensing based on flexible PVDF nanofibers via electro-spinning: a review. Sensors 2018; 18 (2): 330. doi: 10.3390/s18020330

[9] Steffens C, Brezolin AN, Steffens J. Conducting polymer-based cantilever sensors for detection humidity. Scanning 2018; 6: 4782685. doi: 10.1155/2018/4782685

[10] Nambiar S, Yeow JTW. Conductive polymer-based sensors for biomedical applications. Biosensors and Bioelectronics 2011; 26 (5): 1825-1832. doi: 10.1016/j.bios.2010.09.046

[11] Plum TJ, Saxena V, Jessing RJ. Design of a MEMS capacitive chemical sensor based on polymer swelling. In: 2006 IEEE Workshop on Microelectronics and Electron Devices; Boise, ID, USA; 2006. pp. 49-50.

[12] Kumar N, Piccin O, Meylheuc L, Barbé L, Bayle B. Design and modeling of a polymer force sensor. IEEE/ASME Transactions on Mechatronics 2015; 21 (1): 555-564. doi: 10.1109/TMECH.2015.2448662

[13] Pyo S, Lee JI, Kim MO, Lee HK, Kim J. Polymer-based flexible and multi-directional tactile sensor with multiple NiCr piezoresistors. Micro and Nano Systems Letters 2019; 7 (1): 1-20. doi: 10.1186/s40486-019-0085-6

[14] Cheng MY, Lin CL, Lai YT, Yang YJ. A polymer-based capacitive sensing array for normal and shear force measurement. Sensors 2010; 10 (11): 10211-10225. doi: 10.3390/s101110211

[15] Shu Y, Li C, Wang Z, Mi W, Li Y et al. A pressure sensing system for heart rate monitoring with polymer-based pressure sensors and an anti-interference post processing circuit. Sensors 2015; 15 (2): 3224-3235. doi: 10.3390/s150203224

[16] Liu XY, O'Brien M, Mwangi M, Li XJ, Whitesides GM. Paper-based piezoresistive MEMS force sensors. In: 2011 IEEE 24th International Conference on Micro Electro Mechanical Systems; Cancun, Mexico; 2011. pp. 133-136.

[17] Liu X, Mwangi M, Li X, O'Brien M, Whitesides GM. Paper-based piezoresistive MEMS sensors. Lab on a Chip 2011; 11 (13): 2189-2196. doi: 10.1039/C1LC20161A

[18] Ren TL, Tian H, Xie D, Yang Y. Flexible graphite-on-paper piezoresistive sensors. Sensors 2012; 12 (5): 6685-6694. doi: 10.3390/s120506685

[19] Phan HP, Dao DV, Dinh T, Brooke H, Qamar A et al. Graphite-on-paper based tactile sensors using plastic laminating technique. In: 2015 28th IEEE International Conference on Micro Electro Mechanical Systems; Estoril, Portugal; 2015. pp. 825-828.

[20] Crowley K, Nakidde D, Travis J, Agah M. Paper-based MEMS hair cell array. In: SENSORS, IEEE; Baltimore, MD, USA; 2013. pp. 1-4.

[21] Qian Q, Wang Y, Zhang M, Chen L, Feng J et al. Ultrasensitive paper-based polyaniline/graphene composite strain sensor for sign language expression. Composites Science and Technology 2019; 181: 1-20. doi: 10.1016/j.compscitech.2019.05.017

[22] Yu Z, Tang Y, Cai G, Ren R, Tang D. Paper electrode-based flexible pressure sensor for point-of-care immunoassay with digital multimeter. Analytical Chemistry 2018; 91 (2): 1222-1226. doi: 10.1021/acs.analchem.8b04635

[23] Fastier WJ, Dinh T, Dau V, Phan HP, Yang F et al. Low-cost graphite on paper pressure sensor for a robot gripper with a trivial fabrication process. Sensors 2018; 18 (10): 3300. doi: 10.3390/s18103300

[24] Wu Y, Karakurt I, Beker L, Kubota Y, Xu R et al. Piezoresistive stretchable strain sensors with human machine interface demonstrations. Sensors and Actuators A: Physical 2018; 279: 46-52. doi: 10.1016/j.sna.2018.05.036

[25] Stassi S, Cauda V, Canavese G, Pirri C. Flexible tactile sensing based on piezoresistive composites: a review. Sensors 2014; 14 (3): 5296-5332. doi: 10.3390/s140305296

[26] Lin X, Gao S, Fei T, Liu S, Zhao H et al. Study on a paper-based piezoresistive sensor applied to monitoring human physiological signals. Sensors and Actuators A: Physical 2019; 292: 66-70. doi: 10.1016/j.sna.2019.04.009

[27] Turner A, Karube I, Wilson GS. Biosensors: Fundamentals and Applications. New York, NY, USA: Oxford University Press, 1987.

[28] Sanli A, Ramalingame R, Kanoun O. Piezoresistive pressure sensor based on carbon nanotubes/epoxy composite under cyclic loading. In: 2018 IEEE International Instrumentation and Measurement Technology Conference; Houston, TX, USA; 2018. pp. 1-5.

[29] Young WC, Budynas RG, Sadegh AM. Roark's Formulas for Stress and Strain. New York, NY, USA: McGraw-Hill, 2002.

[30] Liu C. Foundations of MEMS. Upper Saddle River, NJ, USA: Prentice Hall, 2012.

[31] Senturia SD. Microsystem Design. Boston, MA, USA: Kluwer Academic Publishers, 2001.

[32] Ayraç T, Gökdel YD. A read-out system for disposable paper-based sensors. In: 2018 3rd International Conference on Computer Science and Engineering; Sarajevo, Bosnia-Herzegovina; 2018. pp. 386-389.

[33] Khan SA, Islam T. Precision active bridge circuit for measuring incremental resistance with ANN compensation of excitation voltage variation. Journal of Sensor Technology 2011; 1 (3): 57-64. doi: 10.4236/jst.2011.13008

[34] Kester W. Practical Design Techniques for Sensor Signal Conditioning. New York, NY, USA: Analog Devices, 1999.

[35] Madzhi NK, Khuan LY, Abdullah MF, Ahmad A. Development of a low cost self-sensing piezoresistive microcantilever biosensor and read-out circuitry for measuring salivary-amylase activity. In: 2010 2nd International Conference on Electronic Computer Technology; Kuala Lumpur, Malaysia; 2010. pp. 9-13.

[36] Anuar AFM, Johari S, Wahab Y, Zainol MZ, Fazmir H et al. Development of a read-out circuitry for piezoresistive microcantilever electrical properties measurement. In: 2015 IEEE Regional Symposium on Micro and Nanoelectronics (RSM); Kuala Terengganu, Malaysia; 2015. pp. 1-4.